3rd International Meeting of the Union for Compact Accelerator-driven Neutron Sources, UCANS III, 31 July–3 August 2012, Bilbao, Spain & the 4th International Meeting of the Union for Compact Accelerator-driven Neutron Sources, UCANS IV, 23-27 September 2013, Sapporo, Hokkaido, Japan

Small angle scattering study of the structure and organization of RNAs and protein of Brome Mosaic Virus (BMV) capsid protein

Narayan Ch. Das[*], Garfield. T. Warren[b], C. Cheng Kao[c], Bogdan G. Dragnea[d], Peng Ni[c], Paul E Sokol[b*]

[a]*Low Energy Neutron Source, Center for the Exploration of Energy and Matter (CEEM), Indian University, IN 47408, USA*
[b]*Department of Physics, Indiana University, IN 47405, USA*
[c]*Department of Molecular and Cellular Biochemistry, Indiana University, Bloomington, IN 47405, USA*
[d]*Department of Chemistry, Indiana University, Bloomington, IN 47405, USA*

Abstract

Brome mosaic virus (BMV) viron is a model system that has a small icosahedral capsid protein (CP) shell. It is well known that BMV is plant virus which is a member of the alpha virus-like superfamily group. These viruses have genetic material and nucleic acids (RNA) with a segmented positive-strand RNA that offers high levels of RNA synthesis and virus production in plants. BMV CP tightly regulates the packaging of its RNAs into the inner core of the capsid while maintaining an outer protein shell coat. Small angle neutron scattering (SANS) and small angle X-ray scattering (SAXS) were applied to study the size, shape and protein-RNAs organization of BMV CP. BMV capsid protein and buffer solution containing a D_2O/H_2O mixture was used to enhance the contrast of the material for neutron scattering measurements. The pair distance distribution $P(r)$ of BMV CP from the indirect Fourier transform of scattering spectrum was able to illustrate the differences in the distribution of materials, signifying RNAs packing, and protein in the BMV CP. The extracted parameter from $P(r)$ shows that the BMV CP is about 260 Å in diameter and is composed of RNA with ~ 74 Å core radiuses and coated protein shell of thickness 56 Å. The contribution of RNAs core, protein shell was estimated by simulation. The contribution due to interference of core and shell called cross term was also extracted from simulation.

* Corresponding author. Tel.: +1-812-855-6183; fax: +1-812-855-5533.
E-mail address: pesokol@indiana.edu.

1. Introduction

Viral particles are biological machines that have evolved to package, protect, and deliver the viral genome into the host via regulated conformational changes of virions. Among different virus, Brome mosaic virus (BMV), a typical spherical plant virus, is one of the simplest entities with four viral proteins and three genomic RNAs. This virus is well suited for analysis of selective encapsidation of RNA [1]. A potential advantage of this encapsidation strategy is to maximize reassortment of the BMV genomes. The BMV virion is a small T= 3 truncated icosahedral of the alpha virus-like superfamily of RNA with a segmented positive-strand RNA genome and a mean diameter ~ 268Å that offers high levels of RNA synthesis and virus production in plants. It infects many species of gramineae and can be easily transmitted mechanically, as well as by various vectors [2]. It is composed of 180 identical copies of the 189-residue coat protein subunit of distinct equal number of either an A, B, C conformation, which contains a long N-terminal arm rich in basic residues and a globular domain that allows subunits to interdigitate through their C-terminal tails, and a multiple genome consisting of tightly regulates two RNAs of 2.1 kb and 0.8 kb designated by RNA3 and RNA4, respectively. Each copy of RNA3 and RNA4 are normally packed together and encapsidated separately within core of the BMV capsid protein (CP) [3, 4]. These BMV CPs are important in many aspects of the viral infection cycle, including modulating gene expression, RNA replication, virus assembly and disassembly.

Plant growth virus has specialization features that make it particularly tractable for certain basic studies and application. BMV CP is an ideal model system and has been studies extensively for both gene regulation and internal virus structure and organization of subunits. Most studies of the physical structure of BMV CP have suggested that only tenuous interactions exist between protein subunits in the capsid, and that virion integrity is maintained principally by protein- RNA interactions. An examination of the structure shows the situation to be somewhat more complicated. Within hexameric capsomeres, but to a considerably lesser extent pentameric capsomeres, subunit interfaces are relatively large and the interactions extensive, comparable to those in other T-3 viruses. The detailed assembly of protein subunits in the capsids of several small RNA virus has investigated by electron microscopy and X-ray/neutron diffraction [5,6]. Very little is known about the RNA and capsid distribution within BMV, revealing that the RNA exists in a shell and that portions of the capsid penetrate into the shell [4]. Indeed, electron microscopy provides no information on the internal structure of small viruses, and low-resolution X-ray/neutron diffraction does not allow unambiguous location or organization of the RNA and proteins. Details quantitative investigation on organization of RNAs and proteins and capsid assembly of the BMV CP and the capsid are still lacking. Therefore, understanding the size, shape and capsid assembly or internal structure of BMV CP represents the first step in understanding whole-virion assembly and may provide new ways of developing antivirals and virus-based therapeutics.

Small angle scattering, either small angle neutron scattering (SANS) or small angle X-ray scattering (SAXS) are ideally suited to characterizing the structure of virus particles in solution because the wavelength are well matched to the length scales being probed which is ranges from 1 to 100 nm [7-9]. While they do not provide structural information at atomic resolution, these techniques are very sensitive to the size and shape of isolated protein/virus and organization or distribution of different subunits into virus and their complex assemblies. SANS has an additional benefit over SAXS since neutron produce far less radiation damage or degradation in most soft biological materials than x-rays. Thus, delicate biological systems may be studied without fear of impacting the results. In addition, while the x-ray scattering length densities of proteins, lipids, and nucleic acids are quite similar, the neutron scattering length densities differ naturally, making it possible to probe the internal structures of virus

particles with SANS [10-12]. SANS has a straight forward ability to contrast match either the RNA or the protein in a simple spherical virus in order to study the organization of the virus. One can achieve the same effect of contrast matching under SAXS by adding sucrose or salts to the buffer; however, one risks problem with swelling or virus dissociation if the ionic strength of the buffer is raised too much. The presence of salt in the buffer does not greatly affect the scattering properties for neutrons. Thus, SANS has an advantage over SAXS; simply by changing the ratio of H_2O to D_2O in the solvent, one can create contrast matching condition, making it much easier to distinguish between protein and hydrated RNAs [13, 14]. The possibility that D_2O may affect the stability or the structure of the virus must be checked in each case, but D_2O is less likely to have and effect than high salt concentrations. This may be useful in future experiment involving protein encapsulation the nanoemulsion droplets.

The size, shape and organization or distributions of protein-RNAs of BMV CP have not yet been systematically studied by small angle scattering method. In this work we have used SANS and SAXS to study the size, shape and protein-RNA organization of plant grown BMV CP. BMV CP in buffer solution with deuterated (D_2O)/hydrogenated water (H_2O) mixture was used to enhance contrast in neutron scattering measurement. The distance distribution function of BMV from the indirect Fourier transform of scattering spectrum gives a clear indication of RNA packing, protein, distribution and their structure in the BMV CP. The result reveals that the virus is about 260 Å in diameter (*D*) and is composed of RNAs with core radius of ~ 74 Å inside the capsid protein shell of thickness ~ 56 Å. The scattering intensity of each RNAs core, capsid protein shell and interference between these two subunits was calculated from distance distribution function of each subunits group. The influence of incoherent background due to presence of large neutron scattering cross-section of hydrogen nuclei on peak resolution has been demonstrated through series of contrast variation calculation.
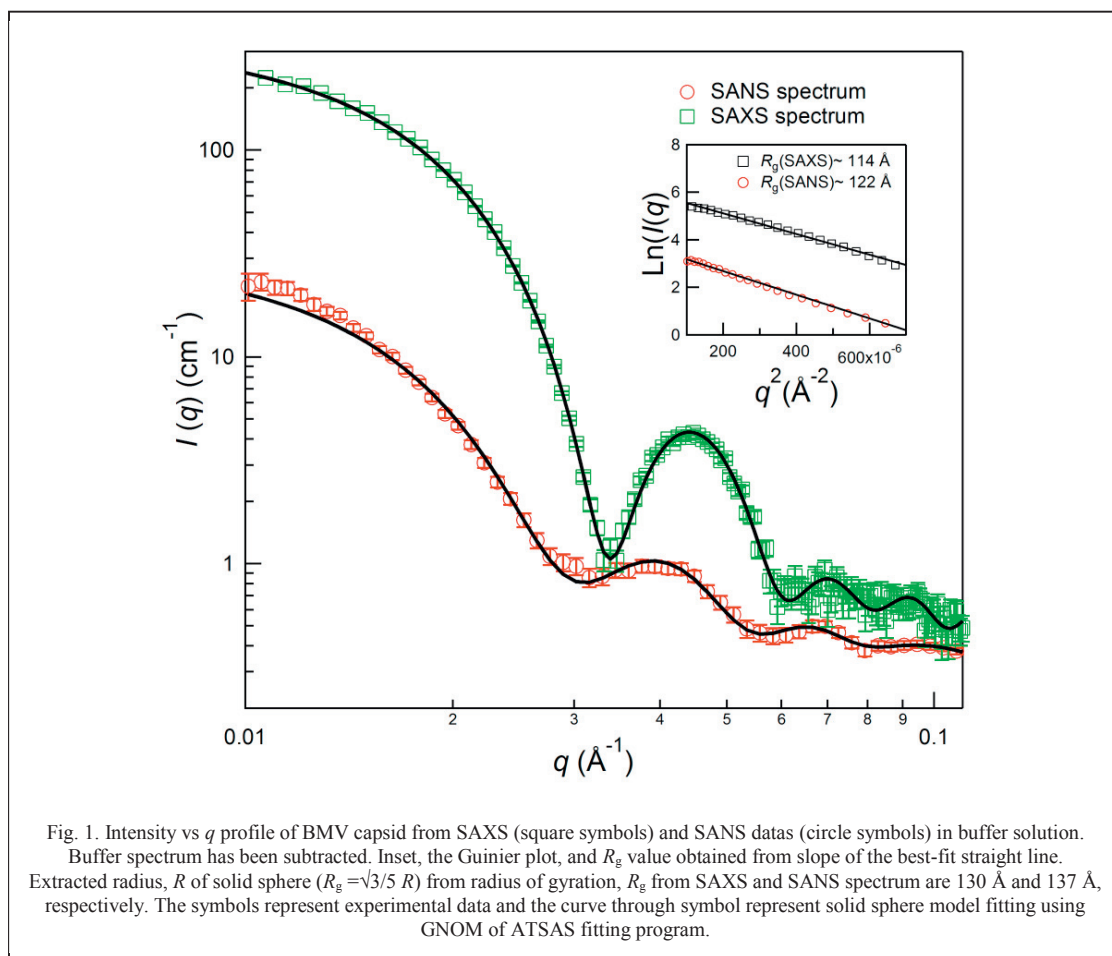
2. Materials and Experimental Techniques

The BMV CP obtained from C. C. Kao group at the Department of Molecular and Cellular Biochemistry, Indiana University, Bloomington. Plant grown BMV CP was mixed in buffer of 50 mM CH_3COONa and 8 mM CH_3COOMg in 87% D2O at pH 5.2. Details synthesis and purification method of BMV CP are reported elsewhere [15,16]

The SAXS patterns of the same BMV sample in buffer and buffer solution were recorded with CuKα radiation from a S-Max 3000 SAXS camera coupled to a RU-200 rotating anode X-ray generator operating at 40 kV and 50 mA (Rigaku) and two-dimensional multi-wire detector. Sample-detector distances of 1.5 m and 0.5 m allowed a "*q* range" from 0.006 to 0.31 Å-1 [$q = 4\pi/\lambda \sin(\theta/2)$, where λ is X-ray wavelength and θ is scattering angle.

The SANS experiments were performed at the Low Energy Neutron Source (LENS) located at the Center for Exploration of Energy and Matter (CEEM), Indiana University. The SANS Instrument at LENS is a conventional neutron 'time-of-flight' instrument. The incident flight path is 8.6 m and uses pinhole collimation to provide a beam with a divergence of 7 mrad at the sample position. A cooled Beryllium filter is used to reduce fast neutron backgrounds and limits the shortest wavelength available to 4 Å. The sample-to-detector distance is variable, from 1.1 – 4.2 m and, for these measurements, 2.2 m was used allowing us to cover a *Q*-range of 0.008 - 0.3 Å^{-1} utilizing λ = 4-10 Å neutrons. For these measurements the accelerator was operated at 13 MeV with a peak current of 20mA, pulse width of 400μS and repetition rate of 20Hz yielding an average power on target of 3 kW. BMV in buffer and buffer solution were prepared in 87/13 D_2O/H_2O, which provides a better neutron scattering contrast between the BMV and the buffer solution. The raw data were circularly averaged after background correction due to sample cell and detector noise and then converted into absolute units by comparison with a water standard, taking into account the transmission of the samples. All measurements were performed at 4^0C. A quartz banjo cell and kapton capillary with a thickness of 2mm was used as sample cell for SANS and SAXS measurement, respectively. All measurements were performed at 4^0C to avoid the lost of the structural integrity of the BMV virus like particles. The neutron flux passing through the sample area of 3.4 cm^2 was around 10^4 n/s The photon flux in SAXS measurement was around 10^8 photon/s and beam size diameter 200 μm The data acquisition times of SANS and SAXS are 40 and 24 hrs.

3. Results and Discussion

The SANS and SAXS profiles of BMV CP particles in buffer [50 mM CH_3COONa and 8 mM CH_3COOMg] in 87% D2O at pH 5.2 is shown in absolute units in Fig. 1. The SANS profiles have a central maximum at a q of 0, followed by three clearly distinguishable subsidiary maxima that are typical of scattering from a predominantly spherical or core-shell spherical particle. The SAXS data shows similar behaviour, although the higher order peaks in SAXS are lost in the noise as a result of the limitation of detector area that provides the data at higher q values. The SAXS profile does show sharper peaks due to higher instrument resolution with respect to the SANS instrument. The SANS spectrum for BMV CP exhibits a large incoherent background due to presence of a large quantity hydrogen nuclei in the sample. X-rays are relatively insensitive to hydrogen and the SAXS spectrum does not exhibit this background. The higher incoherent background in the SANS profile reduces peak resolution or peak heights compared to the peak found in the SAXS profile. The background for the SANS data shown in Fig. 1 is around 0.3 cm^{-1} which is in good agreement with the 87/13 D_2O/H_2O ratio of the buffer solution.

Fig. 1. Intensity vs q profile of BMV capsid from SAXS (square symbols) and SANS datas (circle symbols) in buffer solution. Buffer spectrum has been subtracted. Inset, the Guinier plot, and R_g value obtained from slope of the best-fit straight line. Extracted radius, R of solid sphere ($R_g = \sqrt{3/5}\ R$) from radius of gyration, R_g from SAXS and SANS spectrum are 130 Å and 137 Å, respectively. The symbols represent experimental data and the curve through symbol represent solid sphere model fitting using GNOM of ATSAS fitting program.

The scattering data was analyzed using the Guinier approximation method. This analysis is the most straightforward approach for extraction the radius of gyration, R_g. The Guinier method utilizes a series of expansion of $I(q)$ to derive an approximate Gaussian form $(I(q) = I(0)\ \exp(-q^2 R_g^2/3))$ for the intensity of a monodisperse solution of globular macromolecule. In principle, a linear fit of $\mathrm{Ln}(I(q))$ versus q^2 provides the

intercept and slope, which are related to the $I(0)$, and the R_g, respectively. R_g is a model-independent parameter that provides a measure of the compactness of a particle. An approximate particles size can be estimated from R_g assuming a shape of the virus [17]. Fig. 1 illustrates results obtained from a Guinier fit of the SANS and SAXS data. The extracted R_g values for the BMV particles are shown in the inset in. Although the number of data points in the Guinier region is limited due to the size of virus, the data quality at low q provides small uncertainties, in a relative sense, in the extracted parameters. However, the Guinier plot of the BMV data exhibits good linearity, suggesting that the solution was reasonably free from larger aggregates or strong inter-particles interaction.

To obtain a more detailed picture about size, shape and the distribution of RNA and protein in BMV CP, the pair distance distribution function $P(r)$, R_g and $I(0)$ are extracted through the use of indirect Fourier transform methods. The scattering data was fitted for the distance distribution function, which is the frequency of all pairwise distances within a scattering particle for monodisperse systems, weighted by the scattering-length density difference relative to the solvent. P(r) can be estimated by

$$P(r) = \frac{1}{2\pi^2} \int_0^\infty qr \cdot I(q) \cdot \sin(qr) \cdot dq \tag{1}$$

The evaluated $P(r)$ using the indirect Fourier transform method implemented in the program GNOM (18) are shown in Fig. 2. . The solid curves through the symbols represent the solid sphere model fitting which is used in GNOM program to evaluate the pair distance distribution function. The SAXS spectrum is well fitted with sphere model due to similar electron density of protein and RNAs. The SANS data, in contrast, is not well fit by a single sphere model because of the difference in scattering length density between RNA and the proteins. The maximum linear dimension of the scattering BMV capsid protein, D_{max}, from both SANS and SAXS is 260 Å. The extracted R_g from SANS and SAXS spectrum are 101 Å and 106 Å, respectively. The smaller value for the SANS radius of gyration is due to the higher scattering length density of the RNA that is located in the core of the capsid. The transform (P(r) vs r) of SANS for BMV capsid protein (Figs. 2) showed that there are two regions, ~ 74 Å (core radius) and 130 Å (outer radius), of the BMV CP due to different neutron scattering length of RNAs part and protein part. The results demonstrate that there are differences in the distribution of materials due to variation of contrast between RNA in centre and protein part in the outer shell. Therefore it is confirmed that BMV CP has core-shell sphere shape with core radius ~ 74 Å, which is associated with RNA and shell thickness 56 Å which is associated with protein. The indirect Fourier transform of X-ray data (eqn.1) exhibits single sharp peak which indicates the superposition of two peaks due to similar electron density of protein and RNAs (Fig 2).
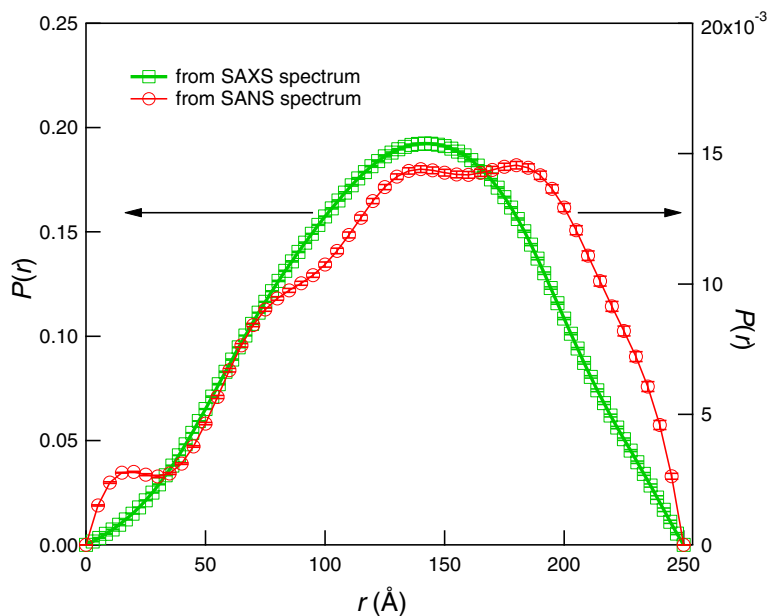
Fig. 2. Distance distribution function, *P*(*r*) evaluated using the indirect Fourier transform method implemented in GNOM program from, SANS (circle) and SAXS (square) profile of BMV capsid protein.

We have also evaluated *P(r)* directly from a numerical model. This allows us to examine separately the contributions from the protein shell, the core RNA and the cross scattering between them. Our model used 2x2x2 Å voxels and directly calculated the chord length between each scattering element. The results are shown in Fig. 3a. The blue line is the result for a sphere (129 Å) with uniform scattering density. This represents the x-ray results since the x-ray scattering length density of the protein shell and the RNA is nearly identical. P(r) for a shell (129 Å OD, 73Å ID) and a sphere (73Å diameter) are represented by the purple and red lines, respectively. There is an additional contribution that must be considered which represents chords that start in the core and end in the shell. This is represented by the black line. The neutrons results will be represented by a average, weighted by the scattering length density, of the core (73Å diameter) associated with RNA packing (red line), shell (56 Å width) associated with protein (purple line), and joint or cross term which is related with interference between core and shell (black line). It is interesting to note the direct contribution from the core is quite small, due to its compact size, while the cross term is comparable in magnitude to that of the shell.
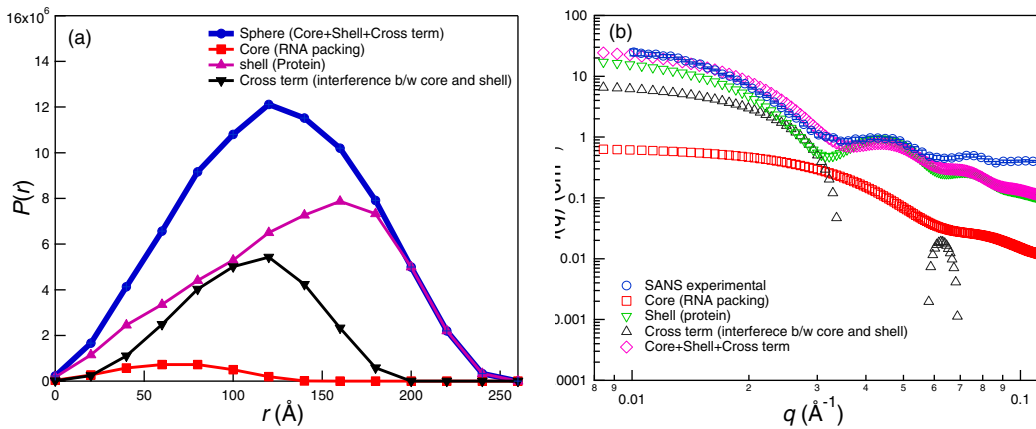
Fig. 3 a)Simulated pair distribution function, $P(r)$ of sphere (protein+RNAs) (129 Å) essentially same with X-ray, core (RNA) (73 Å), shell (from scattering of core of 73 Å and sphere of 129 Å), joint or cross term from interference term between the RNAs and the protein. SANS or SAXS spectrum of BMV capsid protein is the sum of core sphere, shell and cross term or joint related with interference between core and shell. b) The intensity profile of core, shell, cross term calculated from simulated $P(r)$ and sum of these three units. The contrast factor is added to the intensity profile.

The normalized (to unit scattering strength) scattering can be obtained from $P(r)$ using an inverse Fourier transform

$$I_{m,j}(q) = 4\pi \int_{0}^{r_{max}} P_j(r) \frac{\sin(qr)}{qr} dr \qquad (2)$$

where r_{max} is the maximum linear dimension of the scattering particles and q is the momentum transfer. To obtain the measured scattering one must then multiply this normalized scattering by the scattering strength of the component. For a binary complex, like the BMV capsid protein consisting of subunits of RNA and protein having different average scattering-length densities, the scattering is given by:

$$I_{s,c,cs}(q) = (\rho_c - \rho_{sol})^2 I_c(q) + (\rho_s - \rho_{sol})^2 I_c(q) + (\rho_c - \rho_{sol})(\rho_s - \rho_{sol}) I_{cs}(q) \qquad (3)$$

where rc , rs and rsol are scattering length densities of core, shell and solvent, respectively. Ic(q), Is(q) and Ics(q) are the scattering, calculated using eq 2, of the RNA core, the protein shell and the cross term between these two. The measured scattering will also have a contribution from the incoherent scattering from hydrogen in the sample and is given by

$$I(q) = \alpha I_{s,c,cs}(q) + I_{inco.bkg} \qquad (4)$$

where $I_{incoh.bkg}$ is the incoherent background related with D_2O/H_2O and α is a scaling factor.

The neutron scattering length density of RNAs core, protein shell and buffer for this calculation are 2.16×10^{-6}, 1.99×10^{-6} and 2.63×10^{-6} Å^{-2}, respectively. A Simulated scattering intensity calculated from the transform of $P(r)$ of core, shell, and cross term of BMV CP using eqn. 3 are shown in Fig. 3b. These simulated spectrums reveal that the cross term significantly contributes to the small q region (<0.03 Å^{-1}). The small size RNAs core has a minimal contribution while the protein shell has a major contribution to the total scattering spectrums. Comparison of the sum of these terms to the observed scattering, also shown in Fig 3b, shows fairly good agreement. The disagreement at large q is primarily due to the neglect of the incoherent scattering from the buffer and the sample.
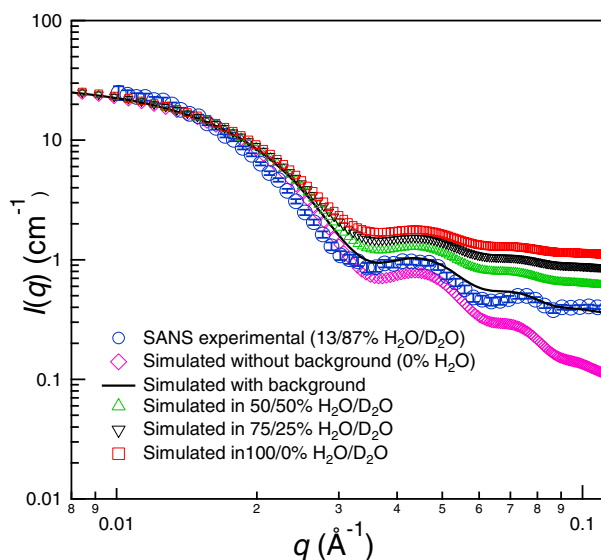
Fig. 4. Simulated contrast variation series in different D_2O/H_2O mixture and experimental intensity profile of BMV CP.

In this report we have utilized SAXS and SANS, at a single buffer concentration, to obtain information on both the core and the shell structure. Our measurements utilized the highest D_2O concentration buffer we could obtain to minimize the contribution of incoherent scattering from H in the sample. This is an important consideration on low intensity sources, such as LENS, where significant data collection times are required to obtain reasonable statistics. In fact, the incoherent component of the scattering places significant limitations on the studies that can be carried out and makes traditional contrast variation techniques difficult to carry out on a LENS-class source.

To explore the effect of incoherent scattering on the observed scattering we have used the *P(r)* above to simulate the scattering in buffer solutions with various D_2O/H_2O concentrations. These are shown in Fig. 4. As can be seen for high D_2O concentrations the oscillations in the observed scattering, which allow us to extract information on the core and shell structure, are quite visible. However, as the H_2O concentration of the buffer is increased these oscillations become less and less visible due to the increase in incoherent scattering. A traditional contrast variation experiment would study the scattering at a variety of different buffer concentrations and would compare results when the contrast matching condition is reached for either the core or the shell. Given the large influence of the incoherent background and the usually small difference in scattering length density between the core and the shell excellent statistics are required to carry out such studies. Thus, they would be extremely difficult to pursue on low intensity sources such as LENS. The much higher flux available at large scale national sources is needed to acquire the required high statistical accuracy data in a reasonable period of time.

4. Conclusion

This study demonstrated that the combination of SANS and SAXS is an efficient tool for proving structural difference between different subunit and gives a fairly clear correlation between the packing of RNAs and protein subunits in BMV or BMV capsid protein particles. This techniques and methodology was successfully used to

elucidate the size, shape and structure of different subunit, such as RNAs as core and protein as shell and interference of core and shell contribution to the spherically core-shell BMV capsid protein. Extracted intensity of RNAs packing, coated protein and interference between RNAs and coated protein confirmed that the interference of core and shell or cross term has significantly contribute to SANS and SAXS spectrum, In addition, the RNAs core has least and protein shell has major contribution to observe scattering spectrum. The methodology presented during this study is broadly applicable to other problems in structural analysis and can provide a new and unique insight into specific structural differences in other virus. Combining SANS studies in heavily deuterated buffers, to minimize incoherent background, with SAXS measurements offers a route for instruments at Compact Accelerator-based Neutron Sources to contribute to biologically important problems.

Acknowledgements

References

[1] Rao LN. Genome packaging by spherical plant RNA viruses. *Annu Rev Phytopathol* 2006;**44**:61–87.
[2] Lane LC. Brome mosaic virus. *CMI/AAB Descript. Plant Viruses*.1977;**180**:1–4.
[3] Ahlquist P, Allison R, Dejong W, Janda M, Kroner P, Pacha R et al. *Molecular biology of bromovirus replication and host specificity*. In Viral Genes and Plant Pathogenesis (T. P. Pirone, J. G. Shaw, eds.), Springer-Verlag, New York;1990, p.144–155.
[4] Jacrot B, Chauvin C, Witz J. Comparative neutron small-angle scattering study of small spherical RNA viruses. *Nature* 1997;**266**:417–421.
[5] Finch JT, Holmes KC, *In Meth Virol* 1967;**3**:351–474.
[6] Jack A, Harrison SC, Leberman R. *J Molec Biol* 1966;**15**: 315-343.
[7] Putnam CD, Hammel M, Hura GL, Tainer JA, X-ray solution scattering (SAXS) combined with crystallography and computation: defining accurate macromolecular structures, conformations and assemblies in solution. *Q Rev Biophys* 2007;**40**: 191–285.
[8] Svergun DI, Small-angle scattering studies of macromolecular solutions. *J Appl Crystallogr* 2007;**40**: S10–S17.
[9] Svergun DI, Koch MHJ. Advances in structure analysis using small-angle scattering in solution. *Curr Opin Struct Biol* 2002;**12**:654–660.
[10] Cuillel M, Berthetcolominas C, Krop B, Tardieu A, Vachette P, Jacrot B. Self-assembly of brome mosaic-virus capsids: kinetic-study using neutron and X-ray solution scattering. *J Mol Biol* 1983;**164**:645–650.
[11] Cusack S, Miller A, Krijgsman PCJ, Mellema JE, An investigation of the structure of alfalfa mosaic-virus by small-angle neutronscattering. *J Mol Biol* 1981;**145**:525–543.
[12] Cusack S, Ruigrok RWH, Krygsman PCJ, Mellema JE, Structure and composition of influenza-virus: a small-angle neutron-scattering study. *J Mol Biol* 1985;**186**:565–582..
[13] Kuzmanovic DA, Elashvili I, Wick C, O'Connell C, Krueger S., Bacteriophage MS2: molecular weight and spatial distribution of the protein and RNA components by small-angle neutron scattering and virus counting. *Structure* 2000;**11**: 1339–1348.
[14] Leimkuhler M, Goldbeck A, Lechner MD, Witz J. Conformational changes preceding decapsidation of bromegrass mosaic virus under hydrostatic pressure: a small-angle neutron scattering study. *J Mol Biol* 2000;**296**:1295–1305.
[15] Yi G, Vaughan RC, Yarbrough I, Dharmaiah S, Kao CC. RNA binding by the brome mosaic virus capsid protein and the regulation of viral RNA accumulation. *J. Mol. Biol.* 2009;**391**:314-326.
[16] Ni p, Wang Z, Ma X, Das NC, Sokol PE, Chiu W, Dragnea B, Hagan M, Kao CC. An examination of the electrostatic interactions between the N-terminal tail of the brome mosaic virus coat protein and encapsidated RNAs. *J Mol Biol*. 2012;**419**:284-300.
[17] Roe RJ, *Method of X-ray and neutron scattering in polymer Science*, Oxford University Press, New York; 2000, p.158-159.
[18] Svergun DI. Determination of the regularization parameter in indirect-transform methods using perceptual criteria. *J Appl Crystallogr* 1992;**25**:495-503.
[19] Ibel K, Stuhrmann HB. Comparison of neutron and x-ray-scattering of dilute myoglobin solutions. *J Mol Biol* 1975;**93**: 255–265.